

# Exit Wave Reconstruction in High-Resolution Electron Microscopy using the Transport of Intensity Equation

Ishizuka K. and Allman B.\*

HREM Research Inc., Matsukazedai, Saitama, 355-0055, Japan and \*IATIA Ltd., Box Hill North, Victoria 3129, Australia  
ishizuka@hremresearch.com

Many samples in electron microscopy are phase objects as in the case of optical microscopy, which means that the phase change of the incident wave is quite strong, while the modulation of amplitude may be negligible. In optical microscopy Zernike phase plate is employed in order to convert the phase modulation into the amplitude modulation that can be recorded as intensity measurement. Unfortunately, it has been difficult to realize an equivalent phase plate in electron microscopy. However, Scherzer [1] showed a simple defocus produces an approximate phase plate in the presence of a spherical aberration (Fig. 1). This imaging technique has been successfully used in electron microscopy.

About twenty years ago, Teague [2] derived an equation, called the Transport of Intensity Equation (TIE), for wave propagation in terms of a phase and intensity and showed that the phase may be determined by measuring only the propagating intensity.

$$\frac{2\pi}{\lambda} \frac{\partial}{\partial z} I(xyz) = -\nabla_{xy} \cdot (I(xyz) \nabla_{xy} \phi(xyz)) \quad (1)$$

In the case of an electron wave this is simply an imaginary part of the Schrödinger equation under the small angle (paraxial) approximation. The TIE was recently applied successfully in medium resolution electron microscopy to observe static potential distributions of biological and non-biological samples or measure magnetic fields. However, there is no application of the TIE for atomic resolution images until recently [3], because it has been believed that an image set obtained with a very small defocus step is required, and therefore signal change may be far below noise level.

## Information transfer

Although the TIE for electrons is accurate enough in theory, we have to consider in practice information transfer achieved by the TIE in the presence of noise. We note that the effect of wave propagation in Fourier space is simply described by a multiplication of a well-known defocus term:

$$\Psi(\mathbf{g}; z_0 + z) = \Psi(\mathbf{g}; z_0) \exp\{-i\pi\lambda z \mathbf{g}^2\} \quad (2)$$

where  $\mathbf{g}$  is a spatial frequency, and a scattering angle is given by  $\alpha = \lambda g$ . Thus, the derivative of the wave function with respect to  $z$  is simply given by

$$\frac{\partial \Psi(\mathbf{g})}{\partial z} = -i\pi\lambda g^2 \Psi(\mathbf{g}, z) \quad (3)$$

Since an image intensity is a product of the complex wave-function and its complex conjugate, we can write down an intensity derivative in Fourier space using the convolution theorem:

$$\begin{aligned} F\left(\frac{\partial I}{\partial z}\right) &= \frac{\partial}{\partial z} F(\psi \cdot \psi^*) \\ &= \frac{\partial}{\partial z} \Psi(\mathbf{g}) \otimes \Psi^*(-\mathbf{g}) + \Psi(\mathbf{g}) \otimes \frac{\partial}{\partial z} \Psi^*(-\mathbf{g}) \\ &= (-i\pi\lambda g^2 \Psi(\mathbf{g})) \otimes \Psi^*(-\mathbf{g}) + \Psi(\mathbf{g}) \otimes (+i\pi\lambda g^2 \Psi^*(-\mathbf{g})) \end{aligned} \quad (4)$$

This clearly indicates that low frequency components will be dumped in proportion to  $g^2$  in the TIE relation. Thus, low frequency will be affected by noise. This non-isotropic information transfer in terms of image frequency is very important feature, when we try to retrieve phase information from the *real* images based on the TIE technique in the presence of noise.

### Evaluation of an intensity derivative

A practical problem of the TIE is we have to evaluate the differential of intensity along the wave propagation direction (z direction) experimentally. An accurate estimate of the intensity differential may be given by a difference of intensities measured at sufficiently close image planes. However, this is not possible in practice due to non-negligible noise on the images. On the other hand, the intensity difference with a large defocus step will give a poor estimate of the differential.

We analyze this problem by using a following Taylor expansion of the intensity with respect to z, the direction of wave propagation:

$$I(xy, z + \varepsilon) = I(xy, z) + \frac{\partial I}{\partial z} \varepsilon + \frac{\partial^2 I}{\partial z^2} \frac{\varepsilon^2}{2!} + \frac{\partial^3 I}{\partial z^3} \frac{\varepsilon^3}{3!} + \frac{\partial^4 I}{\partial z^4} \frac{\varepsilon^4}{4!} + O(\varepsilon^5) \quad (5)$$

It is clear that a simple intensity difference  $I(z + \varepsilon) - I(z)$  between two consecutive planes gives a poor estimate of the derivative, where an error is the first order of the focus distance  $O(\varepsilon)$ .

For the symmetric three-image case, where the three images are recorded with the same defocus distance, the intensity derivative may be given by an intensity difference between the two side planes as follows.

$$\frac{I(z + \varepsilon) - I(z - \varepsilon)}{2\varepsilon} = \frac{\partial I}{\partial z} + O(\varepsilon^2) \quad (6)$$

Here, all of the even order terms of two the Taylor expansions for  $I(z + \varepsilon)$  and  $I(z - \varepsilon)$  are cancelled out, and thus the difference will give the derivative, where an error is the second order of the focus distance. This may be understood when we note that a slope between the two side points exactly gives the derivative of intensity at the center point within the parabolic approximation using three equidistant data points.

### Upper limit of the defocus distance

An upper limit of the defocus distance that gives a good estimate of the derivative thus depends on the number of images used to estimate the derivative. We will estimate the upper limit of the defocus distance by evaluating a residual error term between a derivative and a finite difference formula. For the three-image case the error term is a third order derivative of the intensity as follows

$$O(\varepsilon^2) = \frac{\varepsilon^2}{3!} \frac{\partial^3 I}{\partial z^3} = \frac{\varepsilon^2}{3!} \left( \frac{\partial^3 \psi}{\partial z^3} \cdot \psi^* + \psi \cdot \frac{\partial^3 \psi^*}{\partial z^3} \right) \quad (7)$$

Then, its expression in Fourier space becomes

$$F(O(\varepsilon^2)) = \frac{\varepsilon^2}{3!} \left[ \left[ (-i\pi\lambda g^2)^3 \Psi_g \right] \otimes \Psi_{-g}^* + \Psi_g \otimes \left[ (+i\pi\lambda g^2)^3 \Psi_{-g}^* \right] \right] \quad (8)$$

When we compare this error term with the intensity derivative (4), the error term may be ignored if the following condition is satisfied:

$$(\pi\lambda g_{\max}^2)^2 / 3! \leq c \ll 1 \quad (9)$$

where  $g_{\max}$  is the highest spatial frequency included in the image, and  $c$  is a small number, say 0.25. If this condition is satisfied by the highest spatial frequency, the intensity derivative in real space may also be evaluated with a good accuracy by the difference of the intensities at the two side planes. Our upper defocus limit is 9.5 nm for a resolution of 0.14 nm assuming 400 kV electrons, while the first order approximation indicates 1.0 nm. This large defocus step will give a sufficient change in

intensity even of atomic resolution images. Therefore, the TIE will be applicable even to atomic resolution images as shown in the next section.

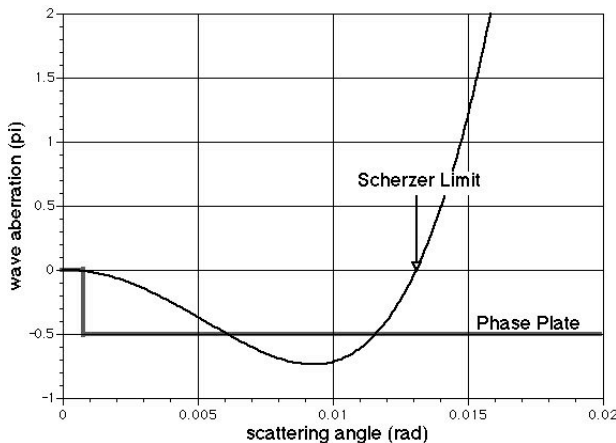
## Results and Discussion

To demonstrate our prediction, we applied the TIE to atomic resolution images of Si<sub>3</sub>N<sub>4</sub>, which was obtained at NCEM [4]. Figure 2 shows a part of three images selected from a through-focus series of twenty images taken with 1.93 nm defocus step. We used here the software, QPt for DigitalMicrograph [5], which was developed based on the algorithm to solve the TIE proposed by Paganin and Nugent [6]. The reconstructed phases at the middle plane without and with low-frequency attenuation are shown in Fig. 3 (a) and (b), respectively. It is evident that very low frequency noise severely affects the reconstructed phase. We can further filter noise contributions using a periodic mask as shown in Fig. 4 (a). We may note that this phase distribution is blurred with a large defocus at the middle plane. Using the phase information at the middle plane, we can propagate the wave back to the specimen exit plane. Figure 4(b) shows the phase distribution at the specimen exit plane, while Fig. 4(c) shows the phase distribution at the plane where an amplitude variation is minimum. Both of the phases shown in Fig. 4 (b) and (c) are remarkably similar to the results reported by Ziegler et al. [4], where all the twenty images were used to reconstruct the phase using the procedure based on Maximum Likelihood [7]

The authors greatly acknowledges Christian Kisielowsky for providing Si<sub>3</sub>N<sub>4</sub> images

## References

- [1] O. Scherzer, J. Appl. Phys. 20 (1949) 20-29.
- [2] M.R. Teague, J. Opt. Soc. Am. 73 (1983) 1434-1441
- [3] K. Ishizuka, B. Allman, J. Electron Microsc. (2004) in press.
- [4] A. Ziegler, C. Kisielowski, R.O. Ritchie, Acta Materialia 50 (2002) 567-574.
- [5] A TIE plug-in for DigitalMicrograph (Gatan), see [www.hremresearch.com](http://www.hremresearch.com) for details.
- [6] D. Paganin, K.A. Nugent, Phys. Rev. Lett. 80 (1998) 2586-2589.
- [7] W.M.J. Coene, A. Thust, M. Op de Beeck, D. Van Dyck, Ultramicroscopy 64 (1996) 109-135.



Wave aberration:

$$\chi(\alpha) = \frac{2\pi}{\lambda} \left\{ \frac{1}{4} Cs\alpha^4 + \frac{1}{2} Z\alpha^2 \right\}$$

**Figure 1:** Pseudo phase plate at the Scherzer conditions. With the presence of a spherical aberration we can realize a phase plate up to the Scherzer limit by adjusting the defocus Z. Here, we assume 200 kV electrons ( $\lambda = 0.0025$  nm) and  $Cs = 0.5$  mm, then  $Z = -43$  nm (under-focus).

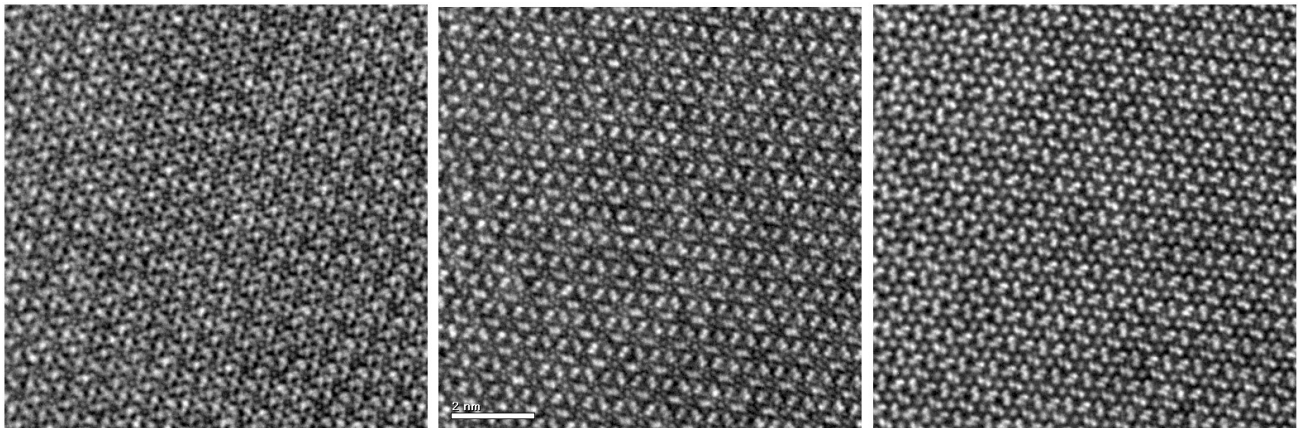


Figure 2: High-resolution images of  $\text{Si}_3\text{N}_4$  obtained at NCEM using a Philips CM300 [4]. Here, we show three images selected from a focal series of twenty images by skipping two images. The defocus of the center image is 273 nm under-focus, and the defocus distance between the under and over-focus images is 11.6 nm. The scale bar is 2 nm. A sampling interval is 0.02 nm.

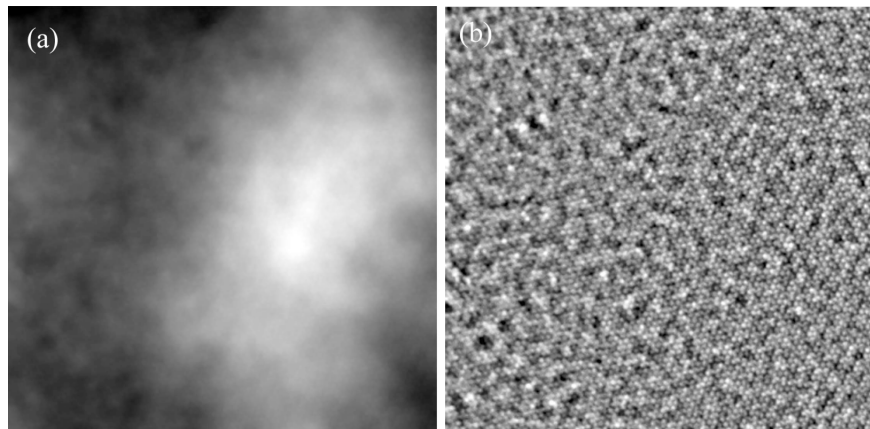


Figure 3: (a) Reconstructed phases as obtained and (b) after low-frequency attenuation. Here, a whole image area of 20 nm is shown. There is a big slowly varying feature, whose phase excursion extends over 55 radians, and the phase variation due to atomic structure is hardly recognized. After low-frequency attenuation the phase map becomes almost flat, and an atomic structure can now be recognized.

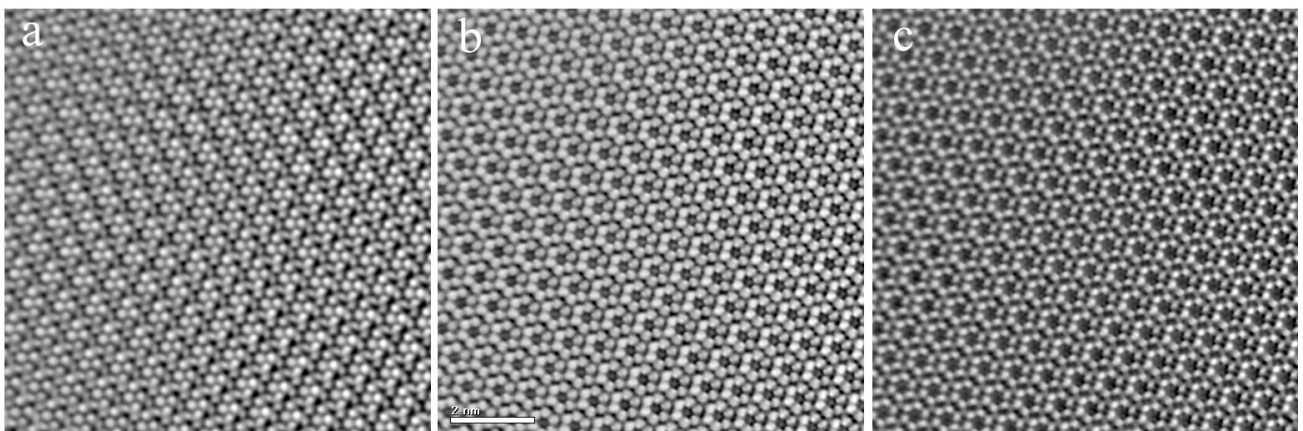


Figure 4: (a) Phase distribution after applying a periodic mask to Fig. 3(b). This is the phase distribution at ca. 270 nm under-focus from the sample. (b) Phase distribution at the specimen exit surface (zero-defocus) obtained by back-propagating the wave front from the observed center image plane. (c) Phase distribution at the plane where an amplitude variation becomes minimum. The phase distribution shown in (c) is more closely related to the structure model than the one shown in (b).